JOURNAL OF MATERIALS SCIENCE 29 (1994) 5499–5514

Review
Cavitation and cavity-induced fracture during superplastic deformation

XING-GANG JIANG*, JAMES C. EARTHMAN, FARGHALLI A. MOHAMED
Materials Section, Department of Mechanical and Aerospace Engineering, University of California, Irvine, CA 92717, USA

The characteristics of fracture by cavitation in superplastic materials are reviewed. Particular attention is paid to the theoretical developmental aspects of cavity nucleation, cavity growth and cavity interlinkage. Various factors, including grain boundary sliding, impurity atoms or particles, phase proportion, deformation temperature, strain rate, strain and grain size, are discussed. Finally, methods for controlling cavitation during superplastic deformation are summarized, and problems which require further work are also presented.

1. Introduction

Most superplastic materials develop internal cavitation during superplastic deformation (SPD) whether they be traditional quasi-single phase materials [1–9], microduplex materials [10–22], or some recently developed advanced materials such as ceramics [23–31], composites [32–35] and intermetallics [36–39]. Cavitation plays an important role in SPD not only for those materials that exhibit final fracture surfaces of substantial area but also for those which pull down to a fine point at fracture. It is recognized that cavitation damage is responsible for the premature failure of several superplastic alloys and excessive cavitation may impose significant limitations on the commercial use of superplastically formed components [40–46]. There is a vast volume of research on this subject which has contributed to an increase in the understanding of the phenomenon. The aim of this paper is to review theoretical aspects of superplastic cavitation and propose some problems which demand further research.

2. Cavity nucleation

2.1. Cavity nucleation models

In this section, it is appropriate to review cavity nucleation models for creep, with the emphasis on the role of grain boundary sliding (GBS) for two reasons. Firstly, superplasticity has been observed in fine-grained materials at temperatures above 0.4 °C of the melting point, where creep also becomes significant. Secondly, well-documented experimental evidence indicates that GBS is a major feature in superplasticity and contributes significantly to the total strain.

Even though cavitation at high temperatures has been studied for several decades the mechanism for cavity nucleation is still not fully understood. Greenwood *et al.* [47] first considered that cavities could nucleate by the continued condensation of vacancies on grain boundaries which experience a normal tensile stress. However, Balluffi and Seigle [48] soon pointed out that the supersaturation of vacancies in the matrix near a grain boundary could be relieved by diffusion to the boundary rather than by precipitation of voids. Intrater and Machlin [49] pointed out that the formation of voids was caused by GBS and that the number of voids produced increased monotonically with the amount of GBS. From this work it appeared that vacancy condensation was not required for cavity nucleation.

Gifkins [50] and Chen and Machlin [51] first proposed that slip impingment produces offsets at the grain boundary which are then opened up as cavities by GBS, as shown in Fig. 1. Chen and Machlin [51, 52] pointed out that any discontinuity in the grain boundary could act as a cavity nucleus. They remarked that the sliding of the grain boundary over a dis-

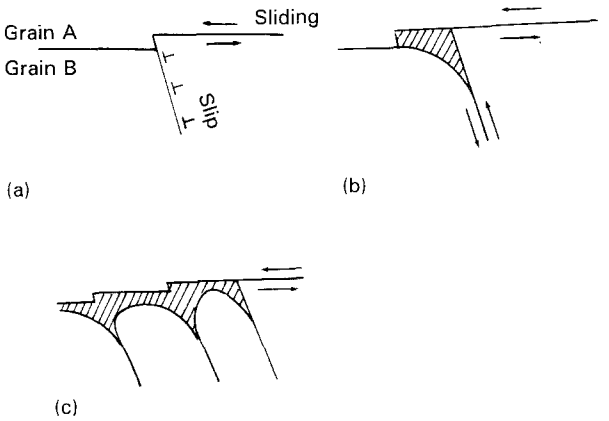

Figure 1 (a) Formation of a grain boundary ledge due to slip [50]; (b) the opening of a cavity due to the combined action of the bulk deformation and GBS; (c) additional cavity formation by a repetition of the process.

* Present address: School of Materials, Science and Engineering, Georgia Institute of Technology, Atlanta, Georgia 30332-0245, USA.

0022–2461

continuity could itself generate a sufficient concentration of stress to cause a void to nucleate. But, Harris [53] noted that the step models were unrealistic because during a sliding burst the cavities would sinter by diffusion immediately after they were formed. Harris [53] calculated the rate of local GBS that must occur for a particle-nucleated cavity of subcritical size to increase its volume by continued sliding after local rupture rather than to sinter together by stress directed diffusion, as shown in Fig. 2. The condition for cavity nucleation is given by

$$v > \frac{D_{gb}\delta}{r^2 \ln \frac{a}{r}}\left(\exp\frac{2\gamma\Omega}{kTr} - 1\right) \quad (1)$$

where v is the grain boundary sliding rate, D_{gb} is the coefficient of grain boundary diffusion, δ is the grain boundary width, r is the radius of curvature of the cavity, a is the radius of the diffusion field of atoms to the void (half the interparticle spacing), γ is the surface energy, Ω is the atomic volume, k is the Boltzmann constant and T is absolute temperature. The problem with Harris's model is that the rate of GBS calculated by Equation 1 is much higher than average measured sliding rates. However, it was demonstrated that macroscopic sliding is not a smooth, continuous process but is characterized by extended periods of zero displacement followed by rapid bursts of sliding many times faster than the overall average [49]. Unfortunately, it is difficult to calculate the exact GBS rate required for cavity nucleation.

Using the concept of classical nucleation theory, Raj and Ashby [54] showed that the stress concentrations set up by GBS can drive vacancies to cluster, thereby forming cavities. Fig. 3 illustrates the model of intergranular cavity nucleation by accommodation of GBS at intergranular particles by diffusion, as proposed by Raj and Ashby. Their model gives the following expression

$$r_c = \frac{2\gamma}{\sigma} \quad (2)$$

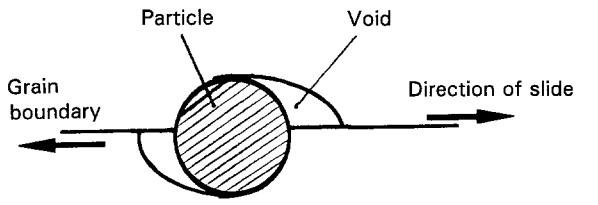

Figure 2 Nucleation of a cavity at a particle on a sliding grain boundary.

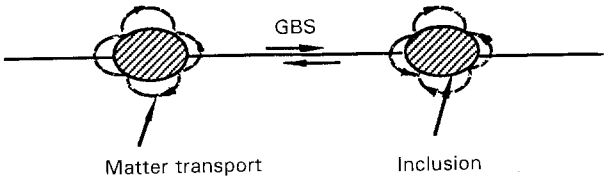

Figure 3 Model of cavity nucleation proposed by Raj and Ashby [54].

where r_c is the critical cavity radius for cavity nucleation, γ is the surface energy and σ is the applied stress. Using the above results, Raj and Ashby proposed a relationship for the cavity nucleation rate of the form

$$\dot{\rho} = \frac{4\pi\gamma}{\Omega^{4/3}\sigma_n} D_{gb}\delta\left(1 + \frac{\sigma_n\Omega}{kT}\right)\left(\rho_{max} - \rho\right) \times \exp\left[-\left(\frac{4r_c^3 F_v}{\sigma_n^2 kT}\right)\right] \quad (3)$$

where σ_n is the normal stress, ρ_{max} is the maximum number of possible nucleation sites per unit area, ρ is the number of cavities per unit area in the grain boundary and F_v is a void shape factor which when multiplied by r_c^3 gives the volume of a critical cavity. The value of F_v is ~ 1 for cavity nucleation at a grain boundary without particles, whereas the value of F_v may be as low as 0.01 for cavity nucleation at apices of grain boundary particles. Generally, the increase in energy for the particle–matrix interface or semi-coherent particles involves a smaller value of F_v, so that nucleation at incoherent or semi-coherent particles has a smaller value of F_v than that for coherent precipitates on grain boundaries. In a subsequent paper, Raj [55] showed in detail that cavity nucleation was possible only above a "threshold" stress and that an incubation period was required to generate vacancy cluster size by atomic and diffusive processes. Generally, the incubation time decreased as the volume of the critical sized vacancy cluster decreased. The role of GBS is to produce stress concentration and thus decrease the incubation time. According to Raj's model, the lower bound for incubation time for vacancies to diffuse and coalesce to form a viable cavity nucleus is

$$t_i = \frac{2\gamma^3 F_v}{\delta D_{gb}\sigma_n^3} \quad (4)$$

The characteristic time for relaxing the high stress concentration by a diffusion process is given by

$$t_d = \frac{(1-\nu^2)\,\gamma_p^3 kT}{2\pi^3 E\delta D_{gb}\Omega} \quad (5)$$

Obviously, the value of t_i should be less than that of t_d for cavities to be nucleated under the stress concentration by GBS. This condition has been found to be satisfied for a copper alloy [55].

Although Raj and Ashby [54] produced a thermodynamic criterion for the stability of the embryo cavity and obtained the critical radius for cavity nucleation, it should be pointed out that the effect of the internal stress has been wrongly assessed where it is given equal importance to the effect of remote stress. The shortcoming of Raj and Ashby's model is that the high strain energy of the stress concentration produced by a pile-up group of dislocations was neglected when the energetics of cavity nucleation was considered.

Argon *et al.* [56] proposed another viewpoint on cavity nucleation. Because very high stresses are needed to cause nucleation to occur at observable rates, they concluded that cavity nucleation is possible

during steady-state creep only when GBS is spasmodic. However, Riedel [57] concluded that sliding-induced cavitation is not possible under usual creep conditions, because the time to relax the high stress concentrations induced by GBS is typically much less than the incubation time for cavity nucleation. Hirth and Nix [58] also noted that the attainment of a state of vacancy supersaturation to cavity nucleation at sites of stress concentration is not easily attainable under usual creep deformation conditions, because the vacancy supersaturation requires long-range diffusion and, hence, a long time.

More recently, Lim [59] proposed a cavity nucleation model at high temperatures involving pile-ups of grain boundary dislocations. Such a model offers an attractive feature, namely, ahead of the pile-up there exists a steady-state stress concentration for cavity nucleation during secondary creep, as shown in Fig. 4. This feature eliminates the problem of the requirement of an incubation time as encountered in Raj and Ashby's sliding model. Lim [59] presented a detailed thermodynamic treatment for cavity nucleation, with emphasis on the respective roles of the remote and local stresses. Lim's analysis demonstrated that the local stresses play only a secondary role and that any effect of sliding is removed within 1 ms after the onset of the GBS event. Lim [60] also extended his grain boundary dislocation pile-up model to address the problem of solute/impurity enhanced cavitation during high temperature deformation. According to Lim's model, it is thus unlikely that cavities are induced by sliding at elevated temperatures.

It is well known that GBS plays an important role in the deformation of superplastic alloys and careful measurements reveal that it contributes more than 50% of the total strain during SPD [61]. Recent experiments have shown that this large GBS contribution remains undiminished even at high superplastic elongations [62]. It is generally considered that cavity nucleation during SPD is caused by a stress concentration at a particle or ledge in the grain boundary produced by GBS. This general conclusion is not in agreement with Lim's model [59].

The stress conditions for the nucleation of cavities or cracks at obstacles due to GBS have been modelled by Smith and Barnby [63] who endeavoured to explain how stress concentrations which were sufficiently large to rupture atomic bonds could arise under conditions of low applied creep stresses. Their model is an outgrowth of the earlier ideas of Stroh [64]. Fleck *et al.* [65] studied the nucleation of cavities at irregular particles in a copper alloy and compared the observed sliding distances between particles with that required by the Smith and Barnby model. They found the sliding distances to be too small to provide decohesion and they suggested that a boundary dislocation pile-up could be increased by addition of a pile-up component in the matrix. Fig. 5a and b illustrates cavity nucleation mechanisms consisting of stress concentrations produced by dislocation pile-ups proposed by Smith and Barnby [63] and Fleck *et al.* [65], respectively. There are two shortcomings in their models, one is that the role of vacancy clustering for cavity nucleation is not considered and the other is that they do not provide a thermodynamic criterion for the stability of the embryo cavity. As a result, the model only gives an upper bound criterion for cavity nucleation.

Very recently, Jiang *et al.* [66] proposed a new cavity nucleation model for high-temperature creep deformation. The authors make the point that cavitation can occur by vacancy clustering where a dislocation pile-up meets a grain boundary, as shown in Fig. 6. Cavity nucleation during creep deformation depends not only on the stress concentration of a pile-up group of dislocations but also on vacancy clustering. The new equation for the critical radius of cavity nucleation is

$$r_c = \frac{2\gamma}{\sigma} - \frac{2d\sigma}{3E} \tag{6}$$

where r_c is the critical radius of cavity nucleation, γ is the surface energy, σ is the remote applied stress, d is the grain size and E is Young's modulus. With the

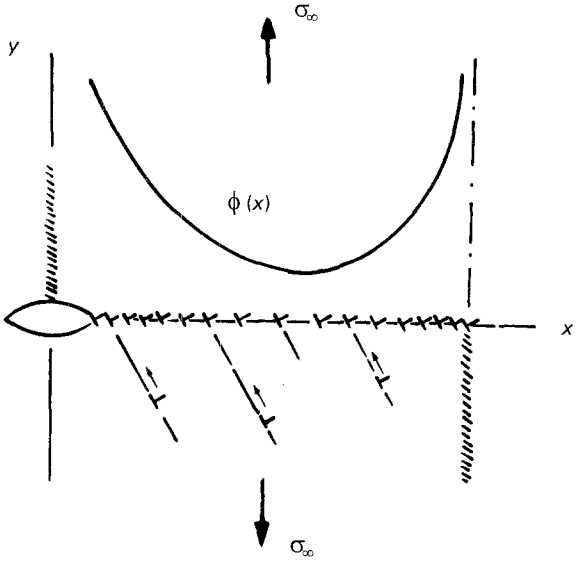

Figure 4 Nucleation of a cavity ahead of a GBS pile-up at the intersection of cell and grain boundaries [59] ; $\phi(x)$ is the distribution function of the GBS in the pile up.

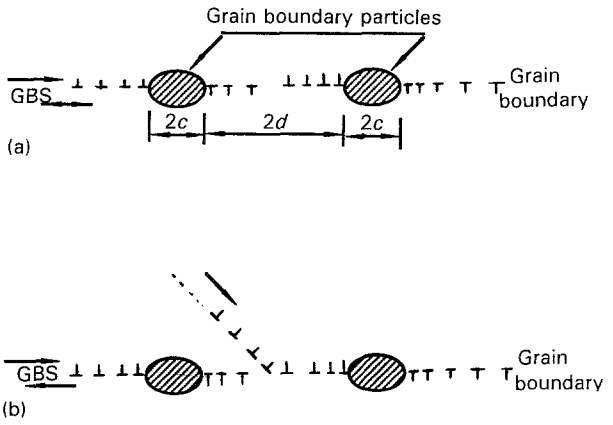

Figure 5 Models of cavity nucleation. (a) Pile-ups of dislocations at particles in a sliding grain boundary [63]; (b) increase in the effective length of a dislocation pile-up by the action of transgranular slip [65].

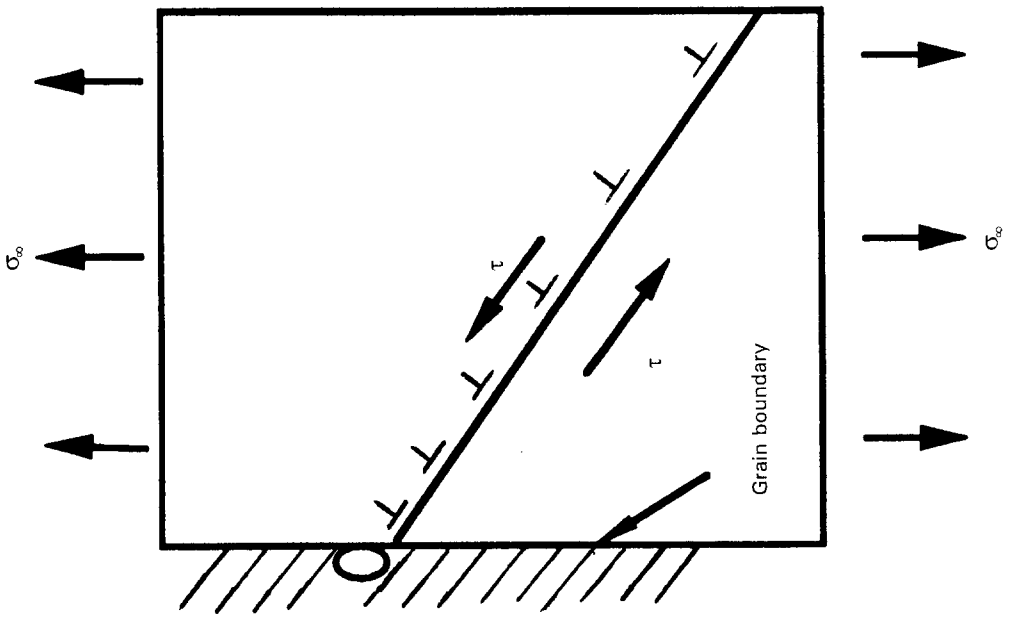

Figure 6 Nucleation of a cavity by vacancy clustering ahead of a pile-up of dislocations [66].

decrease of remote stress, the role of a pile-up group of dislocations is decreased and the role of vacancy clustering for cavity nucleation is increased; when the applied stress is sufficiently small the equation can be simplified to $r_c = 2\gamma/\sigma$, which was proposed by Raj and Ashby [54]. On the other hand, the role of dislocation pile-ups is increased and the role of vacancy clustering is decreased with an increase in the remote stress. In the limit of large applied stresses, the critical radius goes to zero and the upper bound stress for cavity nucleation can be obtained, which is very similar to that proposed by Smith and Barnby [63]. This model brings the vacancy clustering cavity nucleation model, proposed by Raj and Ashby [54], and the stress concentration to rupture atomic bonds cavity nucleation model, proposed by Smith and Barnby [63], together as one equation. The model also addresses the transition condition between the two cavity nucleation models.

Ghosh [1] proposed a dynamic cavity nucleation mechanism for 7475 Al during SPD. He considered that the possible sites for cavity nucleation were all on the particles, and that the distribution of particles was

$$n(r_p) = n_0 e^{-ar_p} \quad (7)$$

where n_0 and a are constants and r_p is the particle radius; the formula indicates that the number of particles which have a radius of r_p is $n(r_p)$. Ghosh assumed that

$$\sigma = 2\gamma/r_p \quad (8)$$

Substituting Equation 8 into Equation 7 gives the distribution of the number of cavities nucleated as

$$n(r_p) = n_0 e^{-2\gamma a/\sigma} \quad (9)$$

The above formula indicates that each particle will correspond to a nucleated cavity.

Although Ghosh's model successfully predicts the increase in the number of cavities with an increase in strain rate, or decrease in temperature, there is a large deviation between theoretical analysis and experimental results. Furthermore, the possibility of cavity nucleation at triple points or ledges was neglected in this model.

2.2. Cavity nucleation sites

During SPD, cavities always nucleate at irregularities along a grain boundary, since high stress concentrations are typically produced at these irregularities. These irregularities are generally considered to be grain boundary particles, grain boundary ledges or steps, and triple junctions. It is also possible for cavity nucleation from pre-existing microvoids, that are introduced during thermomechanical processing, to appear [41, 44–46, 67].

In the following section, cavity nucleation at four sites is discussed: (1) grain boundary particles; (2) grain boundary ledges or steps; (3) triple junctions; and (4) pre-existing microvoids.

2.2.1. Cavity nucleation at grain boundary particles

It has been shown that the particle–matrix interface on sliding grain boundaries is the most likely site for cavities to form [54, 55]. Experimental observations of cavitation in SPD have shown a correlation between the presence of hard second-phase particles and cavitation, particularly for quasi-single phase alloys [1–9]. Needleman and Rice [68] proposed a characterization diffusion length, Λ, over which stress concentrations are rapidly relaxed. This length is assumed to be equal to the critical particle radius over which localized Coble diffusion creep will not relax the large stress concentrations caused by GBS. Accordingly, they proposed that the critical particle radius is given by

$$\Lambda = \left[\frac{\Omega\delta D_{gb}\sigma}{kT\dot{\varepsilon}}\right]^{1/3} \quad (10)$$

where Ω is the atomic volume, δ is the grain boundary width, D_{gb} is the grain boundary diffusion coefficient, k is the Boltzmann constant and T is absolute temperature. The evaluation value of Λ by Equation 10 is twice as large as the largest particles in Al- and Cu-based superplastic alloys. This is not consistent with the occurrence of extensive cavitation in these alloys [69].

Recently, Chokshi and Mukherjee [69] pointed out that the value of Λ may be substantially overestimated if the calculations are performed using the grain boundary diffusion coefficient, since the interphase diffusion coefficient may be several orders of magnitude smaller than the single phase boundary diffusion coefficient. In view of this, Λ may be expressed generally as

$$\Lambda = \left[\frac{\Omega\delta D_{eff}\sigma}{kT\dot{\varepsilon}}\right]^{1/3} \quad (11)$$

where D_{eff} is the effective diffusion coefficient. When the interphase diffusion is rate controlling, Equation 11 reduces to the form given by Equation 10 with D_{gb} being replaced by D_{ib}. If lattice diffusion through the matrix is rate controlling, Equation 11 may be expressed as

$$\Lambda = \left[\frac{\Omega D_l\sigma}{\pi kT\dot{\varepsilon}}\right]^{1/2} \quad (12)$$

Chokshi and Mukherjee [69] used Equation 12 to calculate the critical particle radius for cavity nucleation in Al- and Cu-based superplastic alloys. The results indicate that the critical particle radius below which cavities will not be nucleated are 0.6 and 0.02 μm, respectively ($\dot{\varepsilon} = 10^{-4}\ s^{-1}$). This means there are more potential cavity nucleation sites in the Cu-based alloy as compared with the Al-based alloy, which is verified by many experimental observations [2, 21, 69].

Fleck *et al.* [65] observed that cavity nucleation occurred as a result of dislocation pile-ups at grain boundary particles. In superplastic materials, extensive GBS and pile-ups of dislocations during deformation can lead to a build-up of sufficiently large local stresses around particles resulting in cavity nucleation by a particle–matrix decohesion process. Based on Harris's [53] and Raj and Ashby's [54] calculations for the conditions under which stress concentrations at particles on a grain boundary are relaxed by diffusion, Stowell [41] proposed the critical strain rate formula

$$\dot{\varepsilon}_c = \frac{2.9\sigma\Omega\delta D_{gb}}{\alpha d r_p^2 kT} \quad (13)$$

where $\dot{\varepsilon}_c$ is the critical strain rate below which cavity formation is inhibited by diffusive stress relaxation, α is the fraction of the total tensile strain accommodated by GBS and r_p is the particle radius. Rearranging Equation 13 gives

$$r_p = \left[\frac{2.9\sigma\Omega\delta D_{gb}}{\alpha d\dot{\varepsilon}_c kT}\right]^{1/2} \quad (14)$$

Equation 14 can also be used to estimate the critical particle radius for cavity nucleation. Equations 13 and 14 are consistent with observations of cavities in superplastic aluminum alloys [9, 41].

2.2.2. Cavity nucleation at grain boundary ledges or steps

Experimental results have revealed that grain boundary particles are not always a prerequisite for cavity formation. Grain boundary ledges or steps and triple points can also be cavity nucleation sites, especially for many microduplex alloys, such as Zn–22%Al [21, 69]. Up to now there have been very few theoretical studies of cavity nucleation at grain boundary ledges.

Gifkins [50] first proposed the idea of cavity nucleation at grain boundary ledges. Based on this hypothesis, Chan *et al.* [70] proposed a model for cavity nucleation at grain boundary ledges. The basis of the model is that the probability of cavity nucleation at ledges depends on the relative magnitudes of the incubation period to nucleate cavities and the time necessary to relax stress concentrations by diffusion creep. The model was consistent with experimental observation of ceramics subjected to compressive loads [70].

Recently, based on the principle of Chan *et al.*'s [70] model, Chokshi and Mukherjee [69] developed a model for cavity nucleation at grain boundary ledges during SPD for microduplex alloys. The model assumes that grain boundaries contain ledges with height h and with an inter-ledge separation distance λ. Grain boundaries slide with a characteristic relaxation time, t_{gbs}, leading to the development of stress concentrations at ledges. Cavities may nucleate at grain boundary ledges if the incubation period for cavity nucleation t_i, is less than the characteristic time for the relaxation of stress concentration by localized diffusion creep, t_d.

Using Argon *et al.*'s [56] result, an expression for the characteristic time for GBS, t_{gbs}, is

$$t_{gbs} = \frac{\beta kT\lambda}{\pi b\delta D_{gb}G} \quad (15)$$

where β is a geometrical interaction parameter that depends on h and λ.

Using Chan *et al.*'s [70] result, the characteristic time for the relaxation of a stress concentration by grain boundary diffusion (GBD), t_d, is

$$t_d = \frac{(1-\nu)kTh^3}{4\Omega\delta D_{gb}G} \quad (16)$$

After simplification, Chokshi and Mukherjee [69] obtained a relationship for the characteristic incubation time, t_i, of the form

$$t_i = \frac{250\gamma^3 F_v h^3}{\delta D_{gb}\sigma^3\lambda^3} \quad (17)$$

The general conditions for cavity nucleation at grain boundary ledges is $t_{gbs} < t_i < t_d$.

Combining Equations 15–17 and substituting $1 - \nu = 0.7$ and $\Omega = 0.7b^3$, Chokshi and Mukherjee [69] obtained the condition for cavity nucleation

$$\frac{h}{\lambda} > \left(\frac{\beta kTG^2 h}{250\pi F_v b\gamma^3}\right)^{1/4}\left(\frac{\sigma}{G}\right)^{3/4} \quad (18)$$

and

$$\frac{h}{\lambda} < \left(\frac{kTG^2h^3}{10^3F_v\gamma^3b^3}\right)^{1/3}\left(\frac{\sigma}{G}\right) \quad (19)$$

Chokshi and Mukherjee's [69] analysis shows that cavities may nucleate at grain boundary ledges under a limited set of experimental conditions, as shown in Fig. 7, which may be achieved during the SPD of microduplex alloys.

Although Chokshi and Mukherjee [69] considered the role of GBS for cavity nucleation, the shortcoming of their models is that the grain boundary dislocation pile-up, which may lead up to a build up of sufficiently large local stress around the irregularities, is not considered. In a recent model by Lim [59], it was determined that GBS cannot lead to cavity nucleation at ledges, because the transient stress concentration by sliding is estimated to be less than 1 ms, much smaller than the lower bound incubation time for vacancies to diffuse and coalescence to form a viable cavity nucleus.

2.2.3. Cavity nucleation at triple junctions

It is well accepted that a triple point is another cavity nucleation site during SPD because the stress concentration by GBS at triple points is difficult to relax [44, 45]. For recently developed superplastic 3YTZ, composite 3Y20A and yttria-stabilized tetragonal zirconia ceramics, cavities are often found to nucleate at triple point junctions [24, 25, 28]. For traditional quasi-single phase 7475 Al, 12%Cr–Mo–V steel and microduplex Zn–22%Al, cavities are also typically found at triple junctions [8, 21, 71]. Up to now, there have been very few theoretical analyses that address this phenomenon. However, preferred cavity nucleation at triple junctions is reasonable since stress concentrations develop there as a consequence of GBS.

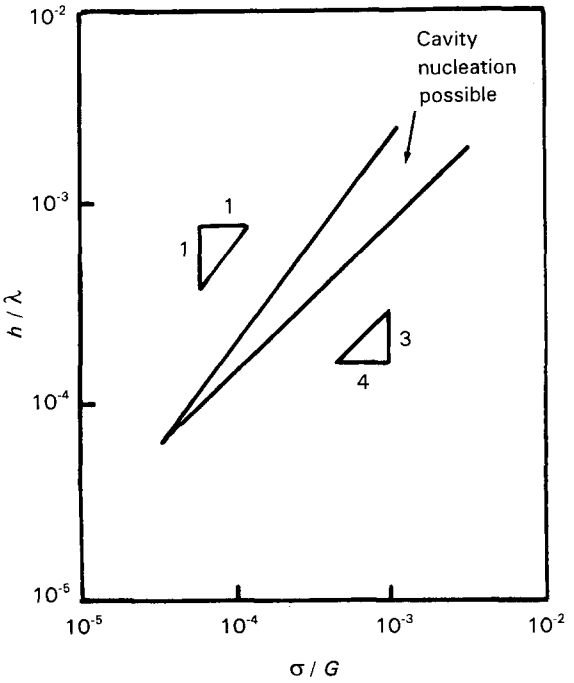

Figure 7 Schematic cavity nucleation map illustrating the limited range of h/λ and σ/G over which cavities may nucleate at grain boundary ledges [69].

2.2.4. The possibility of cavity nucleation from pre-existing microvoids

It has frequently been suggested that cavities may pre-exist in superplastic alloys due to the extensive thermomechanical treatment used to produce the fine grain size [41, 44–46, 67]. Stowell [41, 46] suggested that cavities may pre-exist at zero strain. His analysis predicts that the volume fraction of cavities, Φ, should have an exponential dependence on strain, ε, according to the relationship

$$\Phi = \Phi_0 \ln(\eta\varepsilon) \quad (20)$$

where Φ_0 is the level of cavitation at zero strain and η is a parameter which usually has a value in the range 2–3, but is dependent on the alloy, strain rate, temperature and grain size. Stowell's suggestion is supported by, for example, the microstructural observation of Caceres and Silvetti [67] on a quasi-single phase Zn–22%Al–0.5Cu alloy where it appears that cavities are nucleated at Fe-rich particles in the prior thermomechanical processing.

Recently, Chokshi and Mukherjee [61] pointed out that, since cavity size is typically plotted on a logarithmic scale, an extrapolation of such plots to zero strain will always give a positive offset, irrespective of whether cavities pre-existed or not. Thus, it is noted that, while such plots may be useful in examining the increase in the total level of cavitation damage with strain, they do not provide any evidence for pre-existing cavitation.

It is not possible to rule out the existence of very small voids with dimensions of less than 0.1 μm in numerous microstructural investigations on undeformed superplastic alloys using transmission electron microscopy (TEM), in view of the resolution and sampling limitation of microstructural techniques used. Chokshi and Langdon [21] recently proposed that the time, t, required to remove a void of radius r by sintering during high temperature SPD [21, 69] is given by

$$t = \frac{\phi kTr^4}{\Omega\gamma\delta D_{gb}} \quad (21)$$

where γ is the surface energy and ϕ is a constant having a value of ~ 0.6. The stability of a small cavity before high temperature SPD may be evaluated using the above equation. For example, for microduplex Zn–22%Al [21] and quasi-single phase 7475, or 7075 Al alloy [8, 9], the analytical results show that small pre-existing cavities will sinter rapidly at the elevated temperatures used for SPD. Thus, it is reasonable to assume that cavities do not grow from pre-existing microvoids which may be induced during thermomechanical processing.

2.3. Cavity stringer formation during SPD

A striking feature of cavitation in superplastic materials is the frequent observation of cavities that are

aligned in stringers parallel to the tensile axis [72]. Cavity alignment in stringers was reported in both microduplex alloys, such as Zn–22%Al [19, 21, 73] and quasi-single phase alloys such as 7075 and 7475 Al [9, 74], copper alloys [4, 5, 7, 75–77] and stainless steels [78, 79].

There are still many unanswered questions involving: (1) the mechanism of cavity stringer formation; (2) the effect of strain rate, strain and rolling direction on cavity stringer formation; and (3) the effect of particle stringers on cavity stringer formation.

Van Riet and De Meester [80] first proposed the mechanism for the formation of cavity stringers parallel to the tensile axis. In this mechanism, the sliding of a cluster of grains generates a stress concentration which may be relieved by the formation of a cavity translating the problem of accommodation to another boundary along the side of the sliding cluster. In this way, a row (or stringer) of cavities may develop until the difficulties of accommodation are essentially damped out. However, Van Riet and De Meester's mechanism of cavity stringer formation does not explain why the cavity stringers are aligned to the tensile axis, nor why the cavity stringers are only observed for relatively large superplastic strains.

Recently, Chokshi [72] performed a detailed experimental study on the alignment of cavities in a superplastic commercial copper alloy. He found that cavities were observed to form in stringers parallel to the tensile axis due to cavity nucleation at an aligned stringer of large Co-rich particles present in the as-received alloy. His experimental results indicate that cavity stringers are observed only in specimens exhibiting large elongations to failure. He reasoned that this observation may relate either to an extensive transverse interlinkage of cavities that makes the appearance of stringers obvious or to a requirement of large strain deformation for the actual formation of cavity stringers.

The lack of stringers in specimens exhibiting elongation of $< 400\%$ are consistent with similar observations reported recently by Ma and Langdon [31]. In this paper, the experimental observations showed that there is no evidence for the formation of cavity stringers along the tensile axis for yttria-stabilized zirconia ceramics. This may be due to the fact that these observations were for relatively low strains.

In more recent studies, cavity stringers have also been found in advanced superplastic materials, such as a fine grained yttria-stabilized tetragonal zirconia ceramics [24], and boron-doped Ni_3Al intermetallics [37]. In these materials, optical micrographs reveal that cavities aligned in stringers parallel to the tensile axis. Mukherjee and co-workers [37] proposed that large particles were broken into small pieces and aligned in stringers parallel to the rolling direction while the Ni_3Al was cold rolled to 70%. Subsequently, cavities nucleated at these small particles and resulted in the manifestation of cavities aligned in stringers parallel to the tensile axis.

Another interesting phenomena concerns the effect of the rolling direction on cavity stringer formation. There are two different results for this effect depending on the alloy under investigation. Chokshi and Langdon [7] found that for a quasi-single phase copper alloy containing Co-rich particles, the cavities tended to form in stringers that were always oriented along the rolling direction regardless of the direction of the tensile axis. However, Jiang *et al.* [9] recently found that cavities in the quasi-single phase 7075 Al alloy containing Fe- or Si-rich particles tended to form in stringers that were always oriented along the tensile axis regardless of the rolling direction. The above experimental results indicate that stringers of particles may assist in the formation of cavity stringers in some materials, such as the Cu alloy containing Co-rich particles studied by Caceres and Wilkinson [5] and Chokshi and Langdon [7], but they are not a prerequisite and they are not always responsible for the formation of cavity stringers. For commercial microduplex Zn–22%Al alloys containing impurities higher than 6 p.p.m., it was shown that cavity stringers are always aligned parallel to the tensile stress, regardless of the rolling direction [21, 81]. In this case it can be concluded that cavity stringer formation is in some way caused by the SPD. In summary, an understanding of cavity stringer formation mechanisms is very important because it is a key to the development of methods for predicting and preventing cavity nucleation during SPD.

2.4. Factors that influence cavity nucleation

Cavity nucleation is affected by two types of factors: one is characterized by experimentally imposed factors, such as temperature, strain rate, strain and stress state; the other type is intrinsic to the materials themselves, such as grain size, phase proportions, impurity atoms or particles, grain boundary surface energy. Many of these factors are interdependent. It is not the purpose of this section to discuss all of the factors that influence cavity nucleation that are discussed in the literature [42–45]. Rather, it is of interest here to discuss some apparently conflicting aspects.

2.4.1. GBS

It is well accepted that GBS plays an important role in the deformation of superplastic alloys. For example, careful measurements reveal that GBS contributes more than 50% of the total strain during SPD [82–88], and cavity nucleation is caused by the stress concentrations produced by GBS. Experiments have shown that this large GBS contribution to the total strain remains undiminished even at high superplastic elongations [62]. However, Mayo and Nix [89, 90] suggested that sliding is important only in the initial stages of deformation from the results of their torsion experiments on Pb–62%Sn and Zn–22%Al, and micro-independent studies on Pb–62%Sn. In order to explain the grain shape changes during torsion testing of Sn–38 wt % Pb, they proposed a core-mantle model of SPD in contrast to the sliding-with-accommodation theories envisioned earlier. The basic idea of their model is that two deformation mechanisms operate

simultaneously at different strain rates within a single grain.

Valiev and Langdon [91] and Langdon [92] recently proposed that GBS and the associated relative translation of individual grains represents the dominant deformation mechanism throughout superplastic flow based on an investigation of the role of intragranular dislocation strain in a superplastic Pb–62%Sn eutectic alloy. Furthermore, it was proposed that intragranular dislocation movement occurs only as an accommodation process. Langdon [93] also pointed out that there is an important difference between tension and torsion testing because the area of a longitudinal section will increase during tensile deformation, whereas in torsion the area remains unchanged. Consequently, sliding should be significantly easier in tension than in torsion. Accordingly, the following requires further study:

1. the effect of stress state on the role of GBS in SPD;
2. the effect of GBS on cavity nucleation during superplastic flow.

2.4.2. Impurity atoms and particles

Recent experimental observations of cavitation in superplastic alloys, as well as previous investigations, have indicated that there is a correlation between the presence of impurity atoms or hard second-phase particles and the presence of cavities [2, 5, 7–9, 94–96]. As shown in Fig. 8, there are almost no cavities nucleated over the entire life of ultra-high purity Zn–22%Al [81, 97] during SPD, extensive cavitation is found only in the vicinity of the fracture tip. The addition of impurity atoms leads to the formation of cavities during subsequent deformation, and the more the impurities present the more the cavities nucleated. It was also found that the impurity effect in region I is more obvious than that in region II. This finding is an indirect demonstration of the hypothesis proposed by Mohamed [98], that the presence of the threshold stress in region I is due to the strong segregation of impurity atoms at boundaries and their interaction with grain boundary dislocations.

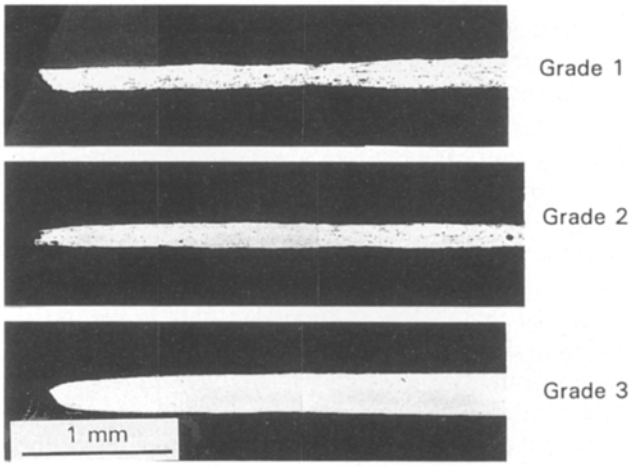

Figure 8 Cavitation in Zn–22%Al grades for $\varepsilon_0 = 1.33 \times 10^{-4} s^{-1}$ [97]. The micrographs correspond to grade 1 (180 p.p.m. of impurities), grade 2 (100 p.p.m. of impurities) and grade 3 (6 p.p.m. of impurities).

Chokshi and Mukherjee [69] have reported that cavities in quasi-single phase alloys are considered to nucleate predominately at coarse grain boundary particles, whereas in microduplex alloys cavities tend to form at interphase boundaries and at triple junctions. Jiang *et al.* [9] have reported TEM observations, shown in Fig. 9, and a theoretical analysis which indicates that the cavities in quasi-single phase high strength aluminum alloys are preferentially nucleated at small particles or irregularities in the grain boundary during SPD. The primary driving force for cavity nucleation is the high stress concentration at discontinuities in the plane of the grain boundary due to GBS. Consequently, the distribution of the particles will have a significant effect on cavity nucleation.

Park and Mohamed [97] have discovered that impurities play an important role in cavity nucleation in microduplex Zn–22%Al alloys. It was found that higher impurity levels gave rise to a greater extent of cavitation, as shown in Fig. 8. The cavity nucleation model by Chokshi and Mukherjee [69], for microduplex alloys, did not consider the role of impurity atoms. It was suggested that the main sites for cavity nucleation are steps or ledges on grain boundaries in microduplex alloys. If this suggestion is correct, cavities will also be nucleated in high purity Zn–22%Al because steps or ledges exist regardless of the impurity content. In fact, cavities are almost never nucleated in ultra-high purity Zn–22% Al [81, 97]. Thus, another cavity nucleation mechanism is needed to account for this finding.

It has been shown in Raj and Ashby's [54] model that the particle–matrix interface on sliding grain boundaries is the most likely site for cavities to form. According to this model, the stress concentration produced by GBS and low surface energies combine to produce the critical cavity volume. According to a recent analysis by Lim [59, 60], the stress concentration produced by GBS should consider the role of grain boundary dislocation pile-ups. It was shown that impurity enhanced cavitation is a complex phenomenon. The findings also indicated that impurities, which are surface active, reduced the boundary diffusivity and decreased the creep resistance of the material, and were most deleterious. These impurities can reduce the threshold stress for cavity failure of the material by about one order of magnitude.

2.4.3. Grain size

It is well recognized that cavity nucleation is decreased by a decreasing grain size. In the superplastic Zn–22% Al alloy, cavitation was found to be minimal when the grain size was less than 5 μm, but increased quite markedly with an initial grain size in excess of 5 μm [73]. Therefore, it appears that cavity nucleation is generally a result of the stress concentrations arising from incomplete accommodations of GBS. In fine grained materials stress concentrations are relatively minor due to the small mean free length (triple point separation) associated with GBS. It was shown in Equation 6 that a decrease in grain size will lead to an

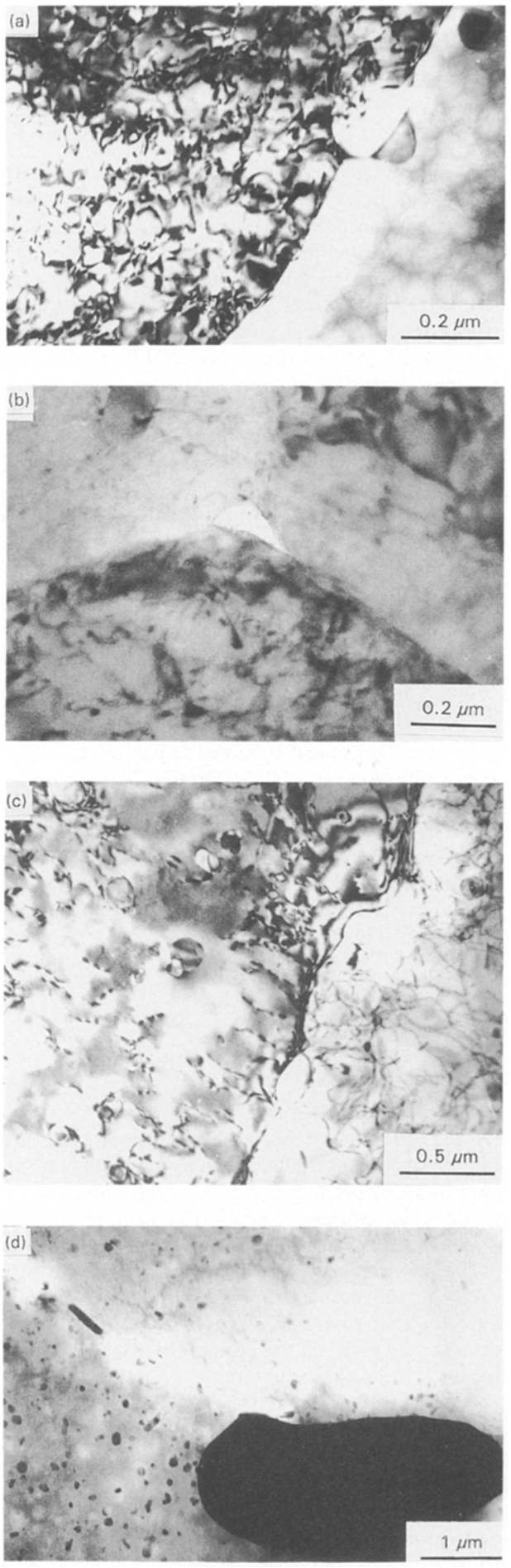

Figure 9 Cavity nucleation in 7475 Al during SPD [8], at: (a) an intergranular particle; (b) a triple junction; (c) a grain boundary ledge; and (d) a large particle in the grain boundary.

increase in the critical radius for cavity nucleation. Generally, grain growth will occur during SPD leading to a continuous increase in the nucleation of cavities during deformation.

It was reported in a recent article by Chokshi [28] that the analytical method by Raj and Ashby [54] will not lead to a reasonable result in superplastic nanocrystalline ceramics. According to their analytical method, the critical radius of cavity nucleation is as follows

$$r_c = \frac{\gamma f(\theta)}{0.7\sigma_n + (\gamma_{gb}/d)} \tag{22}$$

where $f(\theta)$ is a shape factor. The above equation indicates that a decrease in the grain size, d, will lead to a decrease in the size of a stable cavity nuclei, so that cavity nucleation will be facilitated. However, this contradicts the general recognition that cavity nucleation is decreased by decreasing grain size. It seems that a new mechanism of cavity nucleation is needed for nanocrystalline materials.

2.4.4. The effect of strain, temperature and strain rate

The number of cavities generally increases with increasing strain, with the rate of increase depending on both the temperature and strain rate. The stress concentration arising from grain or interphase boundary sliding seems to be at the origin of the formation of the cavities, which are often associated with triple points, hard particles or phases. Increasing the temperature and decreasing the strain rate would reduce cavity nucleation by increasing the time available for diffusional accommodation. The influence of temperature on cavity nucleation is difficult to separate from other parameters, such as grain size and phase proportion, since increasing temperatures lead to an increase in the rate of grain coarsening and a change of the phase proportion for several alloys. It is well known that increasing the volume fraction of the harder phase in a two-phase alloy, such as α/β brass or α/β Cu–Ni–Zn, enhances cavity nucleation [13, 15, 17, 99].

Equation 10 predicts that a decreasing strain rate would reduce cavity nucleation by increasing the time available for diffusional accommodation. According to Equation 6 and $\sigma = c\dot{\varepsilon}^m$ the following is obtained

$$r_c = \frac{2\gamma}{c\dot{\varepsilon}^m} - \frac{2dc\dot{\varepsilon}^m}{3E} \tag{23}$$

where c, d, γ and E are constant for a given material and temperature. The above formula shows that it is possible to reduce cavitation by lowering the strain rate. Such an effect of the strain rate was observed in several alloys [100–102], but, there are also some alloys in which cavity nucleation is independent of strain rate [11, 103, 104]. Furthermore, it was found that a decrease in strain rate led to an increase in the level of cavitation in microduplex steels [105]. In microduplex Zn–22%Al eutectoid it was found that cavitation was of greater importance at very low strain rates [22, 81, 97].

3. Cavity growth mechanisms

The cavity growth mechanisms during high temperature creep deformation have been investigated extensively. Many of these mechanisms are relevant to superplastic alloys. Basically, there are four distinct mechanisms of cavity growth in SPD: (1) stress assisted vacancy diffusion; (2) superplastic diffusion growth; (3) plastic deformation surrounding the cavities; and (4) cavity growth by cavity interlinkage.

3.1. Diffusion controlled cavity growth mechanism

The first important treatment of diffusive cavity growth was given by Hull and Rimmer [106] who showed that the volumetric growth of a grain boundary cavity should be limited primarily by diffusion in the adjoining grain boundary. Subsequently, several models [107–110] were proposed with different modifications and improvements. Two cavities, separated by a distance of $2a$, may grow towards each other by absorbing grain boundary vacancies with the driving force for vacancy flow given by the difference in chemical potential along their common boundary. Speight and Harris [109] derived a relationship for the rate of this cavity growth by diffusion of the form

$$\frac{dr}{d\varepsilon} = \alpha_1 \frac{\Omega\delta D_{gb}[\sigma - (2\gamma/r)]}{2r^2kT\dot{\varepsilon}} \tag{24}$$

where σ is the applied stress, $\dot{\varepsilon}$ is the strain rate, r is the cavity radius and α_1 is a cavity size-spacing term defined as

$$\alpha_1 = \frac{1 - r^2/a^2}{\ln(a/r) - (1 - r^2/a^2)/2} \tag{25}$$

Later, Speight and Beere [107] proposed another relation for this term

$$\alpha_2 = \frac{1}{\ln(a/r) - (1 - r^2/a^2)(3 - r^2/a^2)/4} \tag{26}$$

which is considered to be more complete than that for α_1 [111]. The above cavity growth mechanism has been widely used in SPD assuming a constant value of α_2 [108]. However, recent analysis by Ma and Langdon [111] indicates that the assumption of a constant value of α_2 is reasonable only for large-grained polycrystalline materials and not for superplastic materials where the grain size is typically very small.

3.2. Superplastic diffusion controlled cavity growth

Diffusion models developed to describe cavity growth in coarse-grained alloys undergoing creep deformation consider small cavities which are situated on grain boundaries perpendicular to the tensile axis. There is an enhancement in the diffusional growth of cavities if the cavity size exceeds the grain size since vacancies may diffuse into the cavity along a number of grain boundary paths. Chokshi and Langdon [112] developed a model giving the rate of change of the cavity radius with strain due to superplastic diffusion as

$$\frac{dr}{d\varepsilon} \doteq \frac{45\Omega\delta D_{gb}}{d^2kT}\left(\frac{\sigma}{\dot{\varepsilon}}\right) \tag{27}$$

where r is the cavity radius, ε is the total strain and d is the spatial grain size. A special feature of the above formula is that the change of cavity size with strain is: (1) independent of the instantaneous cavity radius and (2) inversely proportional to the square of the grain size. But there are three limiting conditions for the use of the model: (1) low strain rates; (2) intermediate testing temperatures where vacancy diffusion into the cavities occurs predominantly along grain boundaries rather than through the lattice; and (3) fine grain sizes of the order of $\leqslant 5$ μm. These conditions have restricted the application of the model.

Although this model satisfactorily treats small round individual cavities having radii up to ~ 15 μm [113], it does not consider the interaction and coalescence of adjacent cavities. During SPD the growth of many of the larger cavities involves coalescence. It appears that another model incorporating coalescence is needed to explain cavity growth behaviour during SPD.

Ma and Langdon [114] developed a new model for the growth of an isolated cavity to sizes exceeding the grain size. This model is termed "single cavity superplastic diffusion growth" (SCSPDG). This theory accounts for the multiple fast diffusion paths that are provided by the grain boundaries which intersect the cavity. It leads to a value of $dr/d\varepsilon$ which is proportional to both $1/d$ and to a complex function of r. The model may be important in superplastic ceramics metallics and alloys where the grain size is extremely small.

3.3. Plasticity-controlled cavity growth mechanisms

3.3.1. Hancock's model

During SPD cavities may grow by vacancy condensation controlled by diffusion or by the action of the applied stress producing strains at the surface of the cavity which cause it to grow. The latter mechanism does not involve a vacancy flux to the cavity. Hancock [115] was first to propose the plasticity-controlled cavity growth mechanism. The basic assumption of his model is that cavity growth is controlled by plastic deformation of the matrix around the cavity. His work led to the following equation

$$\frac{dr}{d\varepsilon} = r - \frac{3\gamma}{2\sigma} \tag{28}$$

The first term corresponds to cavity growth by plastic deformation around the cavity and the second term corresponds to the effect of surface tension which tends to shrink the cavity at low stress levels. This equation has been widely used in SPD. It successfully predicts large elongated cavities that form during creep and SPD [115].

3.3.2. Stowell's model

Stowell [116] proposed a semi-empirical plasticity-controlled cavity growth model for fine grained materials during SPD. According to this model the volume fraction of cavities, C_v, during deformation is given by

$$\log\frac{C_v}{C_{v0}} = \mu\varepsilon_m - (\varepsilon_T - \varepsilon_m) \quad (29)$$

where C_{v0} is the initial fraction of cavities at zero strain, ε_m is the deformation far away from the cavity, ε_T is the total deformation and μ is a strain concentration factor taking into account the anisotropy of growth in the direction parallel and perpendicular to the tensile axis. The term $(\varepsilon_T - \varepsilon_m)$ corresponds to the increase in deformation resulting from the presence of the cavities. The value of $\mu \sim 1.5$–3 has been reported for many superplastic alloys.

Based on the models of cavity growth proposed by Hancock [115], Hull and Rimmer [106] and Beere and Speight [107, 108], Stowell [46] proposed a relation for the cavity volume increase rate controlled by plastic deformation of the form

$$\frac{dv}{dt} = \eta v\dot{\varepsilon} \quad (30)$$

where dv/dt is the change rate of cavity volume with time, η is a parameter of cavity growth rate and $\dot{\varepsilon}$ is the true strain rate. Pilling and Ridley [45], based on the results of Cocks and Ashby [117] and Stowell *et al.* [118], found that

$$\eta = \frac{3}{2}\left[\frac{m+1}{m}\right]\sin h\left[2\left(\frac{2-m}{2+m}\right)\left(\frac{k_S}{3} - \frac{P}{\sigma_e}\right)\right] \quad (31)$$

where P is the superimposed pressure, σ_e the equivalent uniaxial flow stress and k_S is a constant. The value of k_S is equal to 1–2 for uni-axial tension, 1.73–2.31 for plain strain and 2–2.5 for bi-axial tension. The value of k_S depends on the extent of GBS during deformation. The lower values represent the case for no GBS whilst the higher values would be valid when the boundaries freely slide. In SPD, k_S values of 1.5 and 2.25 have been adopted for uni- and bi-axial deformations, respectively. The above relationships are in good agreement with experimental data for a wide range of superplastic alloys [45, 118].

3.3.3. Cavitation models for two phase alloys

Belzunce and Suery [14] developed a model of cavity growth by plastic deformation of the soft β-phase surrounding cavities in brass. By assuming a cylindrical cavity whose shape is maintained and by neglecting the effect of the cavity surface energy, the cavity growth rate is

$$\frac{dr}{dt} = \frac{r}{3}\dot{\varepsilon}_\beta = \frac{r}{3g(\alpha)}\dot{\varepsilon}_T \quad (32)$$

where r is the mean equivalent radius, $\dot{\varepsilon}_\beta$ and $\dot{\varepsilon}_T$ are the β-phase strain rate and the total strain rate, respectively, and $g(\alpha)$ is equal to $\dot{\varepsilon}_T/\dot{\varepsilon}_\beta$. Because the proposed model assumes that plastic deformation of the soft β-phase controls the cavitation behaviour in brass, the cavity growth relationship is of the same general form as that usually reported for cavity growth controlled by plastic deformation, i.e.

$$\frac{dr}{dt} = c'r\dot{\varepsilon}_T \quad (33)$$

where c' is a constant with a value close to unity [119].

More recently, Ma and Langdon [120] have utilized a model for crack-like cavity growth to analyse cavitation in an Al–Li alloy; this is important under conditions where the rate of vacancy transport by surface diffusion is not significantly greater than the rate at which vacancies arrive at a cavity tip by GBD. An important difference between diffusion- and plasticity-controlled cavity growth arises from the fact that the former mechanism predicts the rate of change of cavity volume with time to be almost independent of the current volume, where as in the latter mechanism these parameters are proportional to each other.

3.4. Cavity growth models which consider cavity interlinkage

In addition to superplastic materials being capable of resisting neck formation, they also show a remarkable tolerance to the presence of the cavities since cavity volume fractions as high as 30% may be observed in these materials. Many experimental observations show that considerable coalescence of cavities may occur along a direction parallel to the tensile stress before failure occurs.

Stowell *et al.* [118] first developed a cavity growth model considering interlinkage. It was assumed that cavities were spherical in shape and that growth was plasticity controlled. When two cavities touched a large round cavity would immediately form. Pilling [121] developed a cavity growth rate formula using Stowell *et al.*'s result by considering cavity coalescence. He proposed the following equation

$$\frac{\Delta r}{\Delta\varepsilon} = \frac{8V_f\phi(\Delta\varepsilon)\eta[0.13r - 0.37f(r)\Delta\varepsilon] + f(r)}{1 - 4V_f\phi(\Delta\varepsilon)\eta\Delta\varepsilon} \quad (34)$$

where $\phi(\Delta\varepsilon) = [1 + \eta\varepsilon + \eta^2(\Delta\varepsilon)^2/27]$, Δr is the net increase of the mean cavity radius, $\Delta\varepsilon$ is the net increase of true strain and $f(r)$ is the cavity growth rate for which the cavity interlinkage effect is not considered. Based on Pilling's result, Jiang *et al.* [122] proposed a simpler formula for the cavity growth rate which also addresses cavity interlinkage

$$\frac{dr}{d\varepsilon} = f(r) + V_f\eta r \quad (35)$$

If the cavity growth rate before cavity interlinkage is power-law creep controlled then $f(r) = r - 3\gamma/2\sigma$ may be substituted into the above equation, giving

$$\frac{dr}{d\varepsilon} = r(1 + V_f\eta) - \frac{3\gamma}{2\sigma} \quad (36)$$

When the cavity radius becomes sufficiently large the

value of $3\gamma/2\sigma$ in Equation 36 becomes negligible in comparison with the first term, $r(1 + V_f\eta)$. Thus, Equation 36 for small cavities is reduced to

$$\frac{dr}{d\varepsilon} = r(1 + V_f\eta) \quad (37)$$

The above equation represents a much better description of the relationship between V_f, r, η and $dr/d\varepsilon$ in terms of its agreement with experimental results for 7475 Al during SPD [122].

Fig. 10 is a plot of cavity growth rate versus cavity radius for the 7475 Al alloy deformed at 783 K. It can be seen that during the early period of deformation, because the average cavity radius is very small, cavities generally grow according to a diffusion-controlled mechanism. When their radii are larger than 1 μm cavities grow according to the power-law creep mechanism. However, when the cavity radii become sufficiently large the prediction of cavity growth rate by the power-law mechanism gives a value smaller than the measured value. Furthermore, the difference between them increases with increasing cavity size, since the power-law model of cavity growth does not consider the interlinkage of cavities during SPD. The experimental data are more consistent with the new cavity growth rate formula which takes coalescence into account.

Although cavity growth mechanisms during SPD have been investigated extensively, the effect of continuous nucleation of cavities on cavity growth behaviour has not been resolved. Also, all the aforementioned models suggest that cavity shape is regular, although generally the cavity shape is irregular. Finally, the interaction of cavities has been neglected.

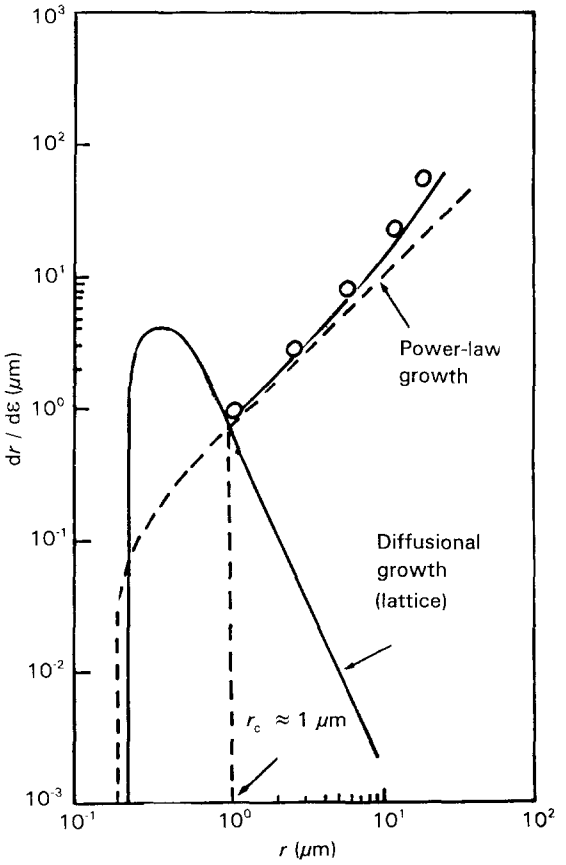

Figure 10 Cavity growth rate versus cavity radius for a 7475 Al alloy deformed at 783 K [122]. —— Theoretical; o—o, experimental; d, 9 μm; σ, 4.5 MPa; $\dot{\varepsilon}_0$, $8.33 \times 10^{-4}\,s^{-1}$.

3.5. Cavity shape changes during SPD

Generally, the shape of cavities formed during SPD will be controlled by the cavity growth mechanism [19, 43–46]. The vacancy diffusion mechanism is favoured at low strains and, as a result, the cavities are approximately spherical and randomly distributed. For high strains the growth is controlled by plastic deformation, and the cavities are more elongated and aligned parallel to the tensile axis. Some cases of intergranular fracture [123] and non-equilibrium diffusion controlled cavity growth have been reported, which apparently corresponds to crack-like cavities.

Recently, Jiang *et al.* [124] applied fractal geometry in describing cavity shape changes during SPD. Because a higher fractal dimension generally corresponds to a more complex cavity shape, the fractal dimension of cavities increases with increasing strain. Hence, the fractal analysis of cavity shape changes provides a method for quantitative analysis of cavity growth during SPD.

3.6. The transitions in rate controlling cavity growth mechanisms

The mechanism by which cavities grow the fastest is the rate controlling mechanism because the cavity growth mechanisms are interdependent [112]. There are two possible transitions that may occur during cavity growth. First, there is a transition from cavity growth controlled by GBD to that controlled by power-law creep. Taking $\alpha_1 = 0.1$ [112] in Equation 24 and combining Equations 24 and 27 gives

$$r_c' = \left(\frac{\Omega\delta D_{gb}\sigma}{5kT\dot{\varepsilon}}\right)^{1/3} \quad (38)$$

where the value of r_c' is the critical cavity radius for the transition from diffusion to power-law cavity growth. When cavity radius $r < r_c'$, cavity growth is controlled by diffusion, and the cavity shape is approximately spherical. But, when $r > r_c'$, cavity growth will be controlled by power-law creep and the cavity shape becomes elongated. The second transition is from cavity growth controlled by superplastic diffusion of grain boundaries to that controlled by power-law creep. Combining Equations 27 and 28

$$r_{csp} = \frac{45\Omega\delta D_{gb}}{kT}\frac{1}{d^2}\frac{\sigma}{\dot{\varepsilon}} \quad (39)$$

where r_{csp} is the critical radius for the transition from superplastic diffusion to power-law cavity growth mechanisms. Fig. 11 shows the variation in the cavity growth rate with cavity radius for the diffusion, superplastic diffusion and plasticity controlled growth mechanisms in a superplastic quasi-single phase Cu alloy [147]. The transition points r_c and r_{csp} are also indicated in the figure.

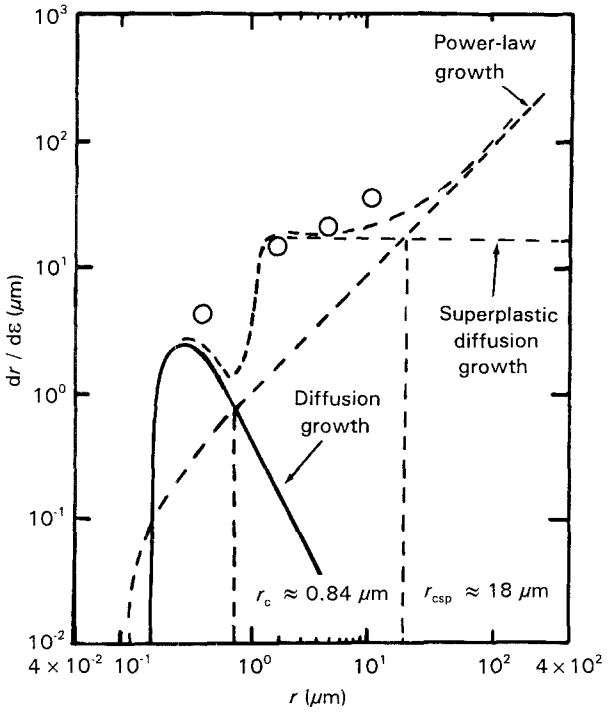

Figure 11 Variation in the cavity growth rate with cavity radius for the diffusion, superplastic diffusion and power-law growth mechanisms [147]. oo, Experimental results; Cu–2.8% Al–1.8% Si–0.4% Co; T, 783 K; d, 2.8 μm; $\sigma/\dot{\varepsilon} = 9.2 \times 10^5$ MPa.

4. Models for predicting the ductility of materials that fail by cavitation

Generally, the greater the strain rate sensitivity, m, the larger the elongation to fracture, δ. There have been many investigations into the relationship between m and δ [125–128]. Unfortunately, all of the models resulting from these studies for predicting δ neglect the effect of cavity nucleation, growth and linkage and are therefore only suitable for materials which are not conducive to cavitation.

4.1. A fractal model for cavity fracture during SPD

Fractals have been widely used in various fields to describe some irregular phenomena in nature since Mandelbrot [129] first proposed fractal geometry. For example, the application of fractals provides an effective tool in the study of highly irregular surfaces [130–139]. It is now generally accepted that the fractal dimension of a fracture surface is a characterization of the roughness of the surface which has potential as a parameter identifying the fracture mechanism.

A fractal model for cavity induced fracture of materials during SPD was recently proposed by Jiang *et al.* [138], based on the fractal concept and the final fracture of the specimen during deformation being due to the tensile stress. A formula which describes the effect of gauge dimensions and grain size of the material on the value of δ was derived. This equation is

$$\delta(\%) = A\frac{\gamma_S h_0 w_0^{2D_F-1}}{n \quad L_0} d^{2(1-D_F)} \qquad (40)$$

where δ(%) is the fracture elongation, A is a parameter correlated with the deformation condition, n is the number of cavities nucleated at a given cross-section of the specimen, γ_S is the fracture surface energy, d is the grain size, D_F is the fractal dimension of the irregular path between cavities that coalesce, and L_0, w_0 and h_0 are the specimen gauge length, width and thickness, respectively. Equation 40 demonstrates that a reduction in grain size results in a larger value of δ. Also, a larger elongation to failure can be obtained by increasing the gauge width and thickness, or by decreasing the gauge length of the specimen. The prediction of the formula is consistent with most experimental results reported to date [140–143].

4.2. Cavity fracture model predicting tensile ductility of superplastic ceramics

In recent years, remarkable developments have occurred in achieving high tensile ductility in ceramic-based materials [144–147]. Ceramic materials having ultrafine-grain sizes (1 μm or less) and have been shown to exhibit high strain rate sensitivity with accompanying high tensile elongations. One of the important features of superplastic ceramics is their capability of exhibiting large elongations to failure in spite of significant concurrent cavitation. This observation is often related to their resistance to transverse cavity interlinkage. Chen and Xue [148] examined the ductility of many superplastic ceramics and they concluded that the elongation to failure is controlled by the flow stress of the material so that although a high strain rate sensitivity is necessary to preclude excessive external flow localization, failure is dominated by the accumulation of internal cavitation damage.

Kim *et al.* [149] examined failure in superplastic ceramics, and they showed that the elongation to failure in superplastic ceramics, ε_f, is given by the following expression

$$\varepsilon_f = K''[\dot{\varepsilon}\exp(Q/RT)/H]^f \qquad (41)$$

where K'' and H are constants, and the exponent $f = -0.33$. Since $\dot{\varepsilon}\exp(Q/RT)$ is proportional to σ, it is clear that the analyses of Chen and Xue [148] and Kim *et al.* [149] relate to stress-controlled cavitation fracture in superplastic ceramics.

Kim *et al.* [149] further proposed a fracture mechanics model which predicts that tensile ductility increases with a decrease in flow stress, a decrease in grain size and an increase in the parameter $2\gamma_S - \gamma_{gb}$. The resulting formula for the elongation to failure is

$$\varepsilon_f = \ln\left\{\left[\frac{(2\gamma_S - \gamma_{gb})E}{\pi C_0}\right]^{1/q}\sigma^{-2/q}\right\} \qquad (42)$$

where C_0 is the initial crack size (normally related to grain size), q is a material constant, possibly related to deformation and intergranular crack growth mechanisms, E is the elastic modulus and σ is the applied tensile stress. The prediction of the above formula has been verified by many experimental observations [149].

5. Sintering of cavitation

Because of the deleterious role of cavitation during SPD, an extensive amount of research has been aimed

at developing ways to restrict or suppress cavitation. There are several possible strategies for restricting cavitation: (1) restricting cavitation before SPD; (2) reducing cavitation during SPD; and (3) removing cavitation after SPD. These strategies are discussed in turn in the following sections.

5.1. Reducing cavitation by annealing prior to SPD

Small cavities can result from the various thermomechanical treatments used to process superplastic materials to obtain a fine grain structure, e.g. rolling and quenching after recrystallization. Varloteaux [150] recently proposed the procedure of reducing cavitation by annealing before SPD. This procedure can homogenize the material further before deformation in order to dissolve complex intermetallic compounds which may melt when the alloy is heated to the deformation temperature. This procedure may also lead to some outgassing of the material. Experimental results of 7475 Al alloys confirm that simple annealing before deformation can significantly reduce subsequent cavity nucleation. But there are two shortcomings of this method; one is that annealing must be performed under vacuum and the other is that grain coarsening is induced during annealing.

5.2. Reducing cavitation by hydrostatic pressure

Experimental observations [44, 45, 151–153] have indicated the following effects of introducing hydrostatic pressure during SPD:

1. decrease the cavity growth rate;
2. decrease the level of cavitation at a given strain;
3. increase the true strain for cavity nucleation;
4. increase the elongation to failure;
5. induce the transition in cavity shape from crack-like to rounded quasi-equilibrium.

It is generally considered that imposing hydrostatic pressure is an effective method of reducing cavitation. Bampton and Raj [151, 152] and Pilling and Ridley [153] found that cavities could be reduced by superimposing hydrostatic pressure during SPD of 7475 Al, 8090 Al–Li alloy and Supral 220 Alloy.

One of the important reasons for imposing hydrostatic pressure during SPD is that it restricts cavity nucleation by increasing the critical cavity nucleation radius. In the case where superimposed hydrostatic pressure, p, is present, σ in Equation 6 has to be replaced by $\sigma - p$, which gives the critical radius as

$$r_c(p) = \frac{2\gamma}{\sigma - p} - \frac{2d(\sigma - p)}{3E} \qquad (43)$$

Comparing Equations 6 and 43, $r_c(p)$ is then larger than r_c for the same stress, σ.

Another important reason for using hydrostatic pressure during SPD is that it restricts cavity growth. In the case where superimposed hydrostatic pressure is present, Equation 31 predicts that the cavity growth rate controlled by plasticity can be reduced by a confining hydrostatic pressure ($P > 0$). This prediction has been verified by experimental results for 7475 Al and an Al–Li alloy [153].

Recently, Conrad *et al.* [154] demonstrated that an externally applied electric field also reduced the level of concurrent cavitation in a superplastic 7475 Al alloy by decreasing the rate of cavity nucleation. The effect of an electric field on cavitation is inferred to result from its promotion of the migration of lattice defects (vacancies and dislocations). This would lead to a more complete accommodation of the stress concentration caused by GBS during SPD.

5.3. Reducing cavitation after SPD

Varloteaux [150] pointed out that annealing can reduce the cavity volume fraction generated during SPD at high temperatures with or without pressure. There are two important considerations for this procedure, one of which is annealing after deformation can sinter only small cavities, otherwise very long times are required. The other consideration is that pressurized annealing can sinter large cavities in a relatively short period of time and can thus be used industrially.

6. Concluding remarks

Much progress has been made in developing an understanding of cavity-induced fracture during SPD. However, there are many questions which remain unanswered. These questions concern the following subject areas.

1. The effect of GBS on cavity nucleation and growth behaviour. Most investigators consider GBS to be the primary deformation mechanisms during SPD. However, an alternative viewpoint based on GBS measurements during torsion experiments suggests that further experimental and theoretical research should be carried out on GBS and its effect on cavitation during SPD.
2. The effect of continuous cavity nucleation on cavity growth behaviour. Not all available cavity growth models consider this effect. However, continuous cavity nucleation is frequently observed during SPD.
3. The mechanism of cavity stringer formation, and whether or not cavities are nucleated from pre-existing microvoids during thermomechanical treatment.
4. The processes involved in cavity nucleation and growth during SPD of advanced ceramics, intermetallics, and composite materials.
5. The effects of impurity atoms and particles on cavity nucleation and growth.

Acknowledgements

This work was supported by the National Science Foundation under Grant No. DMR 902455. Thanks

are extended to Dr K.-T. Park for useful discussions, and to S. L. Hu, Y. Li and S. Yang for their kind help.

References

1. A. K. GHOSH, in "Deformation of polycrystals: Mechanisms and microstructures", 2nd Risø Int. Conf. on Metallurgy and Materials Science, edited by N. Hansen, A. Horsewell, T. Leffers and H. Liholt (Risø National Laboratory, Roskilde, Denmark, 1981) p. 277.
2. C. C. BAMPTON and J. W. EDINGTON, *Metall. Trans.* **13A** (1982) 1721.
3. K. MATSUKI, Y. UENO, M. YAMADA and Y. MURAKAMI, *J. Jpn. Inst. Metals*, **41** (1977) 1136.
4. S. A. SHEI and T. G. LANGDON, *J. Mater. Sci.* **13** (1978) 1084.
5. C. H. CACERES and D. S. WILKINSON, *Acta Metall.* **32** (1984) 423.
6. D. A. MILLER and T. G. LANGDON, *Trans. JIM* **21** (1980) 123.
7. A. H. CHOKSHI and T. G. LANGDON, *Acta Metall. Mater.* **38** (1990) 867.
8. X. G. JIANG, J. Z. CUI and L. X. MA, *Mater. Sci. Engng.* **A157** (1992) 37.
9. X. G. JIANG, J. Z. CUI and L. X. MA, *Acta Metall. Mater.* **41** (1993) 2721.
10. A. H. CHOKSHI and T. G. LANGDON, *J. Mater. Sci.* **24** (1989) 143.
11. D. W. LIVESEY and N. RIDLEY, *Metall. Trans.* **9A** (1978) 519.
12. D. W. LIVESEY and N. RIDLEY, *Metall. Trans.* **13A** (1982) 1619.
13. J. W. D. PATTERSON and N. RIDLEY, *J. Mater. Sci.* **16** (1981) 457.
14. J. BELZUNCE and M. SUERY, *Acta Metall.* **31** (1983) 1479.
15. H. M. SHANG and M. SUERY, *Metal Sci.* **18** (1984) 143.
16. D. W. LIVESEY and N. RIDLEY, *Metal Sci.* **16** (1982) 563.
17. M. SUERY and B. BAUDELET, *Phil. Mag.* **41A** (1980) 41.
18. M. M. I. AHMED, F. A. MOHAMED and T. G. LANGDON, *J. Mater. Sci.* **14** (1979) 2913.
19. D. A. MILLER and T. G. LANGDON, *Metall. Trans.* **9A** (1978) 1688.
20. B. P. KASHYAP and K. TANGRI, *Metall. Trans.* **18A** (1987) 417.
21. A. H. CHOKSHI and T. G. LANGDON, *Acta Metall.* **37** (1989) 715.
22. H. ISHIKAWA, D. G. BHAT, F. A. MOHAMED and T. G. LANGDON, *Metall. Trans.* **8A** (1977) 523.
23. F. WAKAI and H. KATO, *Adv. Ceram. Mater.* **3** (1988) 71.
24. D. J. SCHISSLER, A. H. CHOKSHI, T. G. NEIEH and J. WADSWORTH, *Acta Metall. Mater.* **39** (1991) 3227.
25. A. H. CHOKSHI, *J. Amer. Ceram. Soc.* **74** (1991) 869.
26. K. R. VENKATACHARI and R. RAJ, *J. Amer. Ceram. Soc.* **69** (1986) 135.
27. F. WAKAI, S. SAKAGUCHI and Y. MATSUNO, *Adv. Ceram. Mater.* **1** (1986) 259.
28. A. H. CHOKSHI, *Mater. Sci. Engng. A* **166** (1993) 119.
29. R. DUCLOS, J. CRAMPON and B. AMANA, *Acta Metall.* **37** (1989) 877.
30. T. HERMANNSON, K. P. D. LAGERLOF and G. L. DUNLOP, in "Superplasticity and superplastic forming", edited by C. H. Hamilton and N. E. Paton (TMS-AIME, Warrendale, PA, 1988) p. 631.
31. Y. MA and T. G. LANGDON, in "Superplasticity in metal, ceramics and intermetallics", edited by M. J. Mayo. M. Kobayashi and J. Wadsworth (Materials Research Society, Pittsburgh, PA, 1990) p. 325.
32. M. W. MAHONEY and A. K. GHOSH, *Metall. Trans.* **18A** (1987) 653.
33. A. H. CHOKSHI, D. J. SCHISSLER, T.-G. NIEH and J. W ADSWORTH, in "Superplasticity in metal, ceramics and intermetallics", edited by M. J. Mayo, M. Kobayashi and J. Wadsworth (Materials Research Society, Pittsburgh, PA, 1990) p. 379.
34. F. WAKAI and H. KATO, *Adv. Ceram. Mater.* **3** (1988) 71.
35. T. G. NIEH and J. WADSWORTH, *Acta Metall. Mater.* **39** (1991) 3037.
36. T. G. NIEH, in "Superplasticity in metal, ceramics and intermetallics", edited by M. J. Mayo, M. Kobayashi and J. Wadsworth (Materials Research Society, Pittsburgh, PA, 1990) p. 185.
37. J. MUKHOPADHYAY, G. C. KASCHNER and A. K. MUKHERJEE, in "Superplasticity in aerospace II", edited by Terry R. Mcnelley and H. Charles Heikkenen (TMS-AIME, Warrendale, PA, 1990).
38. T. TAKASUGI, S. RIKUKAWA and S. HANADA, *Acta Metall. Mater.* **40** (1992) 1895.
39. W. B. LEE, H. S. YANG, Y.-W. KIM and A. K. MUKHERJEE, *Scripta Metall. Mater.* **29** (1993) 1403.
40. T. G. LANGDON, *Metal Sci.* **16** (1982) 175.
41. M. J. STOWELL, *Metal Sci.* **17** (1983) 1.
42. N. RIDLEY and J. PILLING, in "Superplasticity", edited by B. Baudelet and M. Suery (Centre Nationale de la Recherche Scientifique, Paris, 1985) p. 8.1.
43. M. SUERY, in "Superplasticity", edited by B. Baudelet and M. Suery (Centre Nationale de la Recherche Scientifique, Paris, 1985) p. 9.1.
44. B. P. KASHYAP and A. K. MUKHERJEE, *Res. Mechanica* **17** (1986) 293.
45. J. PILLING and N. RIDLEY, *Res. Mechanica* **23** (1988) 31.
46. M. J. STOWELL, in "Superplastic forming of structural alloys", edited by N. E. Paton and C. H. Hamilton (TMS–AIME, Warrendale, PA, 1982) p. 321.
47. J. N. GREENWOOD, D. R. MILLER and J. W. SUITER, *Acta Metall.* **2** (1954) 250.
48. R. W. BALLUFFI and L. L. SEIGLE, *Acta Metall.* **3** (1955) 170.
49. J. INTRATER and E. S. MACHLIN, *Acta Metall.* **7** (1959) 140.
50. R. D. GIFKINS, *Acta Metall.* **4** (1956) 98.
51. C. W. CHEN and E. S. MACHLIN, *Acta Metall.* **4** (1956) 655.
52. C. W. CHEN and E. S. MACHLIN, *Trans. Met. Soc.* **209** (1957) 829.
53. J. E. HARRIS, *Trans. Met. Soc.* **233** (1965) 1509.
54. R. RAJ and M. F. ASHBY, *Acta Metall.* **23** (1975) 653.
55. R. RAJ, *Acta Metall.* **26** (1978) 995.
56. A. S. ARGON, I.-W. CHEN and C. W. LAU, in "Creep fatigue environment interactions", edited by R. M. Pelloux and N. S. Stoloff (AIME, New York, 1980) p. 46.
57. H. RIEDEL, *Acta Metall.* **32** (1984) 313.
58. J. P. HIRTH and W. D. NIX, *Acta Metall.* **33** (1985) 359.
59. L. C. LIM, *Acta Metall.* **35** (1987) 1663.
60. L. C. LIM, *Acta Metall.* **37** (1989) 969.
61. A. H. CHOKSHI and A. K. MUKHERJEE, in "Superplasticity and superplastic forming", edited by C.H.Hamilton and N. E. Paton (TMS–AIME, Warrendale, PA, 1988) p. 149.
62. Z. R. LIN, A. H. CHOKSHI and T. G. LANGDON, *J. Mater. Sci.* **23** (1988) 2712.
63. E. SMITH and J. T. BARNBY, *Metal Sci. J.* **1** (1967) 1.
64. A. N. STROH, *Proc. R. Soc.* **A232** (1955) 548.
65. R. G. FLECK, D. M. R. TAPLIN and C. J. BEEVERS, *Acta Metall.* **23** (1975) 415.
66. X. G. JIANG, J. Z. CUI and L. X. MA, *Acta Metall. Mater.* **41** (1993) 539.
67. C. H. CACERES and S. P. SILVETTI, *Acta Metall.* **35** (1987) 897.
68. A. NEEDLEMAN and J. R. RICE, *Acta Metall.* **28** (1980) 1315.
69. A. H. CHOKSHI and A. K. MUKHERJEE, *Acta Metall.* **37** (1989) 3007.
70. K. S. CHAN, R. A. PAGE and J. LANKFORD, *Acta Metall.* **34** (1986) 2361.
71. G. EGGELER, J. C. EARTHMAN, N. NILSVANG and B. ILSCHNER, *Acta Metall.* **37** (1989) 49.
72. A. H. CHOKSHI, *Metall. Trans.* **18A** (1987) 63.
73. D. W. LIVESEY and N. RIDLEY, *J. Mater. Sci.* **17** (1982) 2257.
74. M. G. ZELIN, H. S. YANG, R. Z. VALIEV and A. K. MUKHERJEE, *Metall. Trans.* **24A** (1993) 417.

75. A. H. CHOKSHI and T. G. LANGDON, in "Superplasticity", edited by B. Baudelet and M. Suery (CNRS, Paris, 1985) p. 2.1.
76. T. KAINUMA, A. ARIELI and A. K. MUKHERJEE, in "Deformation of polycrystals: Mechanisms and microstructures", edited by N. Hansen, A. Horsewell, T. Leffers and H. Lilholt (Risø National Laboratory, Roskilde, Denmark, 1980) p. 315.
77. W. J. CLEGG, J. A. ROOUM and A. K. MUKHERJEE, in "Strength of metals and alloys", Vol. 2, edited by R. C. Gifkins (Pergamon Press, Oxford, 1983) p. 689.
78. C. I. SMITH and N. RIDLEY, *Metals Tech.* **1** (1974) 191.
79. C. W. HUMPHRIES and N. RIDLEY, *J. Mater. Sci.* **9** (1974) 1429.
80. C. VAN RIET and P. DE MEESTER, *Scripta Metall.* **9** (1985) 795.
81. K. T. PARK, SUSAN YANG, J. C. EARTHMAN and F. A. MOHAMED, *Mater. Sci. Engng* (in press).
82. R. B. VASTAVA and T. G. LANGDON, *Acta Metall.* **27** (1979) 251.
83. D. L. HOLT, *Trans. AIME* **242** (1968) 25.
84. D. LEE, *Acta Metall.* **17** (1969) 1057.
85. K. MATSUKI, Y. UENO and M. YAMADA, *J. Jpn. Inst. Metals* **38** (1974) 219.
86. O. A. KAIBYSHEV, R. Z. VALIEV and V. V. ASTANIN, *Phys. Status Solidi (A)* **35** (1976) 403.
87. K. MATSUKI, H. MORITA, M. YAMADA and Y. MURAKAMI, *Metal Sci.* **11** (1977) 156.
88. I. I. NOVIKOV, V. K. PORTNOY and T. E. TERENTIEVA, *Acta Metall.* **25** (1977) 1139.
89. M. J. MAYO and W. D. NIX, *Acta Metall.* **36** (1988) 2183.
90. M. J. MAYO and W. D. NIX, *Acta Metall.* **37** (1989) 1121.
91. R. Z. VALIEV and T. G. LANGDON, *Acta Metall. Mater.* **41** (1993) 949.
92. T. G. LANGDON, *Mater. Sci. Engng.* **A166** (1993) 67.
93. T. G. LANGDON, *Mater. Sci. Engng.* **A137** (1991) 1.
94. D. W. LIVESEY and N. RIDLEY, *J. Mater. Sci.* **13** (1978) 825.
95. C. I. SMITH, B. NORGATE and N. RIDLEY, *Metal Sci.* **10** (1976) 182.
96. D. J. LIOYD and D. M. MOORE, in "Superplastic forming of structural alloys", edited by N. E. Paton and C. H. Hamilton (TMS–AIME, Warrendale, PA, 1982) p. 147.
97. K.-T. PARK and F. A. MOHAMED, *Metall. Trans.* **21A** (1990) 2605.
98. F. A. MOHAMED, *J. Mater. Sci.* **18** (1983) 582.
99. M. SUERY and B. BAUDELET, in "Superplastic forming of structural alloys", edited by N. E. Paton and C. H. Hamilton (TMS–AIME, Warrendale, PA, 1982) p. 105.
100. S. SAGAT, P. BLENKINSOP, and D. M. R. TAPLIN, *J. Inst. Metals* **100** (1972) 268.
101. G. L. DUNLOP, E. SHAPIRO, D. M. R. TAPLIN and J. CRANE, *Metall. Trans.* **4** (1973) 2039.
102. S. SAGAT and D. M. R. TAPLIN, *Acta Metall.* **24** (1976) 307.
103. N. RIDLEY, D. W. LIVESEY and A. K. MUKHERJEE, *J. Mater. Sci.* **19** (1984) 1321.
104. N. RIDLEY, D. W. LIVESEY and A. K. MUKHERJEE, *Metall. Trans.* **15A** (1984) 1443.
105. C. W. HUMPHRIES and N. RIDLEY, *J. Mater. Sci.* **9** (1974) 1429.
106. D. HULL and R. E. RIMMER, *Phil. Mag.* **4** (1959) 573.
107. M. V. SPEIGHT and W. BEERE, *Metal Sci.* **9** (1975) 190.
108. W. BEERE and M. V. SPEIGHT, *Metal Sci.* **12** (1978) 172.
109. M. V. SPEIGHT and J. E. HARRIS, *Metal Sci. J.* **1** (1967) 83.
110. A. H. CHOKSHI, *J. Mater. Sci.* **21** (1986) 2073.
111. Y. MA and T. G. LANGDON, *Scripta Metall. et Mater.* **26** (1992) 1239.
112. A. H. CHOKSHI and T. G. LANGDON, *Acta Metall.* **35** (1987) 1089.
113. D. A. MILLER and T. G. LANGDON, *Metall. Trans.* **10A** (1979) 1869.
114. Y. MA and T. G. LANGDON, *Mater. Res. Soc. Symp. Proc.* **196** (1990) 39.
115. J. W. HANCOCK, *Metal Sci.* **10** (1976) 319.
116. M. J. STOWELL, *Metal Sci.* **14** (1980) 267.
117. A. C. F. COCKS and M. F. ASHBY, *Metal Sci.* **16** (1982) 465.
118. M. J. STOWELL, D. W. LIVESEY and N. RIDLEY, *Acta Metall.* **32** (1984) 35.
119. J. W. HANCOCK, *Metal Sci.* **12** (1978) 172.
120. Y. MA and T. G. LANGDON, in "Superplasticity and superplastic forming", edited by C. H. Hamilton and N. E. Paton (TMS–AIME, Warrendale, PA, 1988) p. 173.
121. J. PILLING, *Mater. Sci. Tech.* **1** (1985) 461.
122. X. G. JIANG, J. Z. CUI and L. X. MA, *Mater. Sci. Engng.* **A174** (1994) L9.
123. R. G. FLECK, C. J. BEEVERS and D. M. R. TAPLIN, *Metal Sci.* **9** (1975) 49.
124. X. G. JIANG, J. Z. CUI and L. X. MA, *Mater. Res. Soc. Symp. Proc.* **196** (1990) 373.
125. W. B. MORRISON, *Trans. Met. Soc. AIME* **242** (1968) 2221.
126. M. A. BURKE and W. D. NIX, *Acta Metall.* **33** (1975) 793.
127. E. W. HART, *Acta Metall.* **15** (1967) 351.
128. LIU QIN, *Metall. Trans.* **17A** (1986) 685.
129. B. B. MANDELBROT, "The fractal geometry of nature" (Freeman, New York, 1983).
130. B. B. MANDELBROT, D. E. PASSOJA and A. L. PAULLAY, *Nature, Lond.* **308** (1984) 721.
131. C. S. PANDE, L. E. RICHARDS, N. LOUAT, B. D. DEMPSEY and A. J. SCHOEBLE, *Acta Metall.* **35** (1987) 1633.
132. K. BANERJI, *Metall. Trans.* **19A** (1988) 961.
133. J. C. M. LI, *Scripta Metall.* **22** (1988) 837.
134. R. H. DAUSKARDT, F. HAUBENSAK and R. O. RITCHIE, *Acta Metall. Mater.* **38** (1990) 143.
135. K. K. RAY and G. MANDAL, *Acta Metall. Mater.* **40** (1992) 463.
136. X. G. JIANG, *J. Mater. Sci. Lett.* **11** (1992) 1379.
137. X. G. JIANG, W. Y. CHU and C. M. HSIAO, *Acta Metall. Mater.* **42** (1994) 105.
138. X. G. JIANG, J. Z. CUI and L. X. MA, *Acta Metall. Mater.* **40** (1992) 1267.
139. X. G. JIANG, J. Z. CUI and L. X. MA, *J. Mater. Sci. Lett.* **12** (1993) 1618.
140. F. A. MOHAMED, M. M. I. AHMED and T. G. LANGDON, *Metall. Trans.* **8A** (1977) 933.
141. T. G. NIEH and J. WADSWORTH, *Scripta Met. Mater.* **24** (1990) 763.
142. P. SHARIAT and T. G. LANGDON, in Proceedings of the ISTFA 1985, ATFA, Torrance, CA, 1985, p. 289.
143. K. HIGASHI, T. OHNISHI and Y. NAKATANI, *Scripta Met.* **19** (1985) 821.
144. T. G. LANGDON, *JOM* **42** (1990) 8.
145. O. D. SHERBY and J. WADSWORTH, *Progr. Mater. Sci.* **33** (1989) 169.
146. T. G. NIEH and J. WADSWORTH, *Acta Metall. Mater.* **39** (1991) 3037.
147. A. H. CHOKSHI, A. K. MUKHERJEE and T. G. LANGDON, *Mater. Sci. Engng.* **R10** (1993) 237.
148. I.-W. CHEN and L. A. XUE, *J. Amer. Ceram. Soc.* **73** (1990) 2585.
149. W. J. KIM, J. WOLFENSTINE and O. D. SHERBY, *Acta Metall. Mater.* **39** (1991) 199.
150. A. VARLOTEAUX, J. J. BLANDIN and M. SUERY, *Mater. Sci. Tech.* **5** (1989) 1109.
151. C. C. BAMPTON and R. RAJ, *Metall. Trans.* **13A** (1982) 1721.
152. C. C. BAMPTON and R. RAJ, *Acta Metall.* **30** (1982) 2043.
153. J. PILLING and N. RIDLEY, *Acta Metall.* **34** (1986) 669.
154. H. CONRAD, W. D. CAO, X. P. LU and A. F. SPRECHER, *Mater. Sci. Engng.* **A138** (1991) 247.

Received 7 January
and accepted 8 March 1994